Korean J. Chem. Eng., **30**(2), 448-455 (2013)
DOI: 10.1007/s11814-012-0126-9

Adsorption ability of oxidized multiwalled carbon nanotubes towards aqueous Ce(III) and Sm(III)

Fattaneh Naderi Behdani*, Alireza Talebizadeh Rafsanjani*,†, Meisam Torab-Mostaedi, and Seyed Mohammad Amin Koochaki Mohammadpour***

*School of Chemical Engineering, University College of Engineering, University of Tehran, P. O. Box 11365-4563, Tehran, Iran
**Nuclear Fuel Cycle Research School, Nuclear Science and Technology Research Institute, P. O. Box 11365-8486, Tehran, Iran
(*Received 16 May 2012 • accepted 2 August 2012*)

Abstract−The aim of the present work was to investigate the adsorption of Ce(III) and Sm(III) onto multiwalled carbon nanotubes (MWCNTs) oxidized with concentrate nitric acid. The effects of solution pH, adsorbent dosage, and contact time were studied by batch technique. Langmuir, Freundlich and D-R isotherms were used to describe the adsorption behavior of Ce(III) and Sm(III) by oxidized MWCNTs, and the experimental results fitted Freundlich model well. The maximum uptake capacities (q_m) calculated by applying the Langmuir equation for samarium and cerium ions were found to be 89.28 and 92.59 (mg/g), respectively. A comparison of the kinetic models and the overall experimental data was best fitted by the pseudo second-order kinetic model. The calculated thermodynamic parameters (ΔG^o, ΔH^o, and ΔS^o) showed that the adsorption for Ce(III) and Sm(III) is feasible, spontaneous and exothermic at 30-60 °C. Moreover, more than 70% of Ce(III) and Sm(III) adsorbed onto Oxidized MWCNTs could be desorbed with HNO_3.

Key words: Multiwalled Carbon Nanotubes (MWCNTs), Cerium, Samarium, Adsorption, Desorption, Isotherm, Kinetics

INTRODUCTION

Lanthanides are widely used in the field of nuclear energy, metallurgy, electronics, chemical engineering, and computers and the demand for them has increased correspondingly and is expected to correspondingly increase in time [1,2]. Cerium, as the most abundant and one of the members of the group, has some well established uses that are quite different from the others. However, high purity is usually required for its industrial applications, where it is used, for example, for sulfur control in steels, ceramic, catalyst support, pyrophoric alloys, publishing powders, etc. Cerium is accompanied by other rare earth elements in its minerals, as well as in the spent nuclear fuel [3]. Samarium-153 is a beta emitter with a half-life of 46.3 hours. It is used to kill cancer cells in the treatment of lung cancer, prostate cancer, breast cancer and osteosarcoma [4]. Another important application of samarium and its compounds is as catalyst and chemical reagent. But it has been reported that cerium and samarium have some toxicity. For example, cerium is a strong reducing agent that ignites spontaneously in air at 65 to 80 °C and fumes from cerium fires are toxic [5]. And the soluble salts of samarium are slightly toxic.

The lanthanides elements are the important fission product isotopes which are produced from irradiated nuclear fuel. The environmental behavior of lanthanides has received great interest in environmental impact assessment of disposed long-lived radioactive waste [6]. In view of the toxicity and in order to meet regulations of safe discharge standards, it is essential to remove lanthanides from wastewaters/effluents before it is released into the environment. A number of technologies have been developed over the years to remove toxic metals from wastewater. Conventional methods for the removal of to remove lanthanide ions from wastewater include ion-exchange, solvent extraction, chemical precipitation, membrane filtration and electrochemical treatment [7].

However, all these conventional methods have some disadvantages such as high consumption of reagent and energy, low selectivity, high operational cost and generation of secondary pollutants [8]. In contrast, adsorption could be the most cost-effective for metal removal due to easy operation, high efficiency over a wide concentration range and low secondary pollution with suitable regeneration operation [9]. The key to the adsorption process lies in the selection of appropriate adsorbent. Although various materials such as calcium alginate beads [10], leaf powder [11,12], and biomass [13] have been used as adsorbents in the last few years, there are still some problems in their applications, including the impurities in the adsorbents, slow adsorption kinetics, low adsorption capacities and complex regeneration. Consequently, alternative materials with high sorption rate and increased capacities for metal ions are particularly desired [14].

Carbon nanotubes (CNTs) are novel and interesting graphitic carbon materials which have attracted great interest in many areas since their discovery by Iijima in 1991 [15]. CNTs include single-walled carbon nanotubes (SWCNTs) and multi-walled carbon nanotubes (MWCNTs), depending on their number of layers [16]. CNTs have been proven to possess excellent adsorption capacity in removal of heavy metal ions, radionuclides and organic pollutants [17-21] from

†To whom correspondence should be addressed.
E-mail: atalebi@ut.ac.ir

large volumes of aqueous solutions because of their high specific surface area, their unique porous and hollow nanosize structures. However, the cost of the other adsorbents is lower than the MWCNTs; it is expected that because of possibility of adsorption - desorption of MWCNTs and reusability of them, costs can be reduced. Although adsorption of heavy metal ions on different kinds of MWCNTs has been studied, the adsorption mechanism of lanthanides on MWCNTs is still not clear.

In this work, the adsorption of Ce(III) and Sm(III) from aqueous solution by oxidized MWCNTs is studied as the function of pH, adsorbent dosage and contact time. Langmuir, Freundlich and D-R isotherms and three kinetic models were applied to fit the experimental data. The desorption of Ce(III) and Sm(III) from oxidized MWCNTs was also studied.

MATERIALS AND METHOD

1. Material

All the chemicals used in the study were of analytical (AR) grade. Stock solutions of cerium and samarium (1,000 mg/L) were prepared by dissolving $Ce(NO_3)_3 \cdot 6H_2O$ and $Sm(NO_3)_3$ in double distilled water. The stock solution was then diluted with distilled water to obtain the different concentrations of Ce(III) and Sm(III) for the adsorption experiments.

2. Preparation and Oxidation of MWCNTs

As-prepared MWCNTs with outer diameter of less than 10 nm and length 5-10 μm, which were kindly provided by Qinhuangdao, China, were immersed into a flask containing concentrated nitric acid solution (65%, Merck) and were refluxed for 2 h at 140 °C to remove the impurity and modify surface functionally. After cooling, the MWCNTs were washed using double distilled water several times until pH of the washing water showed no change, then dried at 110 °C for 24 h, then the oxidized MWCNTs were obtained.

3. Characterization of Adsorbent

The scan electron microscope (SEM) images of initial and oxidized MWCNTs are observed by using a model S4160 (FESEM HITACHI JAPAN) and the transmission electron microscope (TEM) images of as-prepared and oxidized MWCNTs are observed by using a model CM120 (PHILIPS). The transmission FTIR measurements were performed using a Fourier transform spectrometer (Bruker Vector 22) in the wave number range of 500-4,000 cm^{-1}.

4. Adsorption

The adsorption of samarium and cerium on oxidized MWCNTs was studied by using the batch procedure. The experiments were repeated twice and the mean values were taken into account. For each experimental run, 50 mL aqueous solution of known concentration of Ce(III) and Sm(III) was taken in round-bottom flasks containing determined amount of oxidized MWCNTs. These flasks were agitated at a constant rate of 200 rpm in a temperature controlled shaker. The initial pH of each solution was adjusted to the desired value with 0.1 M HNO_3 or NaOH solution. The effect of initial pH on the sorption was studied by adjusting the pH in the range of 2-8.

The effect of oxidized MWCNTs dosage on Ce(III) and Sm(III) removal was studied by using 20 mg/L initial Ce(III) and Sm(III) concentration in conjunction with 0.2, 0.4, 0.6, 0.8, 1, 1.2 g/L MWCNTs oxidized. Samples were taken at the times 5, 10, 15, 20, 30, 40, 50, 60, 75, 90 and 120 min to determine optimal contact time. The initial concentrations were adjusted to 10, 20, 50, 75, 100, 150 and 200 mg/L to investigate adsorption isotherm models of the sorption process. The sorption studies were also carried out at 30, 40, 50 and 60 °C to determine the effect of temperature and to evaluate the sorption thermodynamic parameters. After each experiment, the samples were filtered using 0.45 μm filters (Whatman) and the metal concentration of solution was analyzed by inductively coupled plasma-atomic emission spectroscopy (ICP-AES), using a model Varian Liberty 150AX.

The amounts of metal ions per unit of adsorbent at time t (q_t, mg/g) and at equilibrium (q_e, mg/g) were calculated by using Eqs. (1) and (2), respectively.

$$q_t = \frac{(C_0 - C_t) \times V}{M} \tag{1}$$

$$q_e = \frac{(C_0 - C_e) \times V}{M} \tag{2}$$

Where C_0 is the initial ion concentration (mg/L), C_t is the concentration of ion at t time (mg/L), C_e is the equilibrium ion concentration (mg/L), V is the volume of solution (L) and M is the mass of adsorbent.

The removal percentage of Samarium and Cerium was calculated for each run by the following expression:

$$\text{Adsorption } (\%) = \left(\frac{C_0 - C_f}{C_0}\right) \times 100 \tag{3}$$

Where, C_f is the final ion concentration (mg/L).

The average absolute value of relative error, AARE, is used to compare the predicted results with the experimental data. This is defined as follows:

$$\text{AARE} = \frac{1}{\text{NDP}} \sum_{i=1}^{NDP} \frac{|\text{Predicted value} - \text{Experimental value}|}{\text{Experimental}} \tag{4}$$

In which NDP is the number of data points.

5. Desorption

For desorption studies, 40 mg of Oxidized MWCNTs was initially contacted with 50 ml of 20 mg/L metal ion solution at pH 5.0. After equilibrium adsorption, the equilibrium concentration (C_e) of metal ion was measured. The solutions were filtered using 0.45 μm filters to recover the MWCNTs samples. These MWCNTs were dried at 70 °C and dispersed into 50 mL distilled water and shaken for 2 h. Then the pH of the solution was adjusted to the range of 1.55-4.0. Finally, the equilibrium concentration after desorption (C_d) was measured. The percentage of desorption D (%), was calculated by:

$$D(\%) = \frac{C_d}{C_0 - C_e} \times 100 \tag{5}$$

RESULTS AND DISCUSSION

1. Characterization of MWCNTs

Table 1 presents the BET surface area, pore volume and pore diameter of the MWCNTs before and after oxidization. Increase in the structural parameters is shown after oxidization. This treatment is known to remove the amorphous carbon and catalyst particles, make better dispersion of the MWCNTs, break the intertube spaces and

Table 1. Surface characteristics of the materials studied

Sample	S_{BET} [m^2 g^{-1}]	V_p [cm^3 g^{-1}]	D_p [nm]
MWCNTs	97.48	0.098	4
MWCNTs-ox	151.7	0.278	7.3

S_{BET}: BET surface area; V_p: pore specific volume; D_p: pore diameter

even open the tips partially.

The scan electron microscope (SEM) images of initial and oxidized MWCNTs are presented in Fig. 1. It is observed that the isolated MWCNTs usually curve and have cylindrical shapes with diameters of 70-150 nm. The MWCNTs oxidized with HNO_3 are uniform in size, but have smaller diameters and more surface than the untreated CNTs.

The transmission electron microscope (TEM) images of as-prepared and oxidized MWCNTs are shown in Fig. 2. As can be observed, a large amount of metal catalysts and amorphous carbon appeared within as-prepared MWCNTs and was removed after oxidation.

The FTIR spectra for the MWCNTs are presented in Fig. 3. For both materials, the bands in the spectrum at 3,440, 1,629 cm^{-1} are

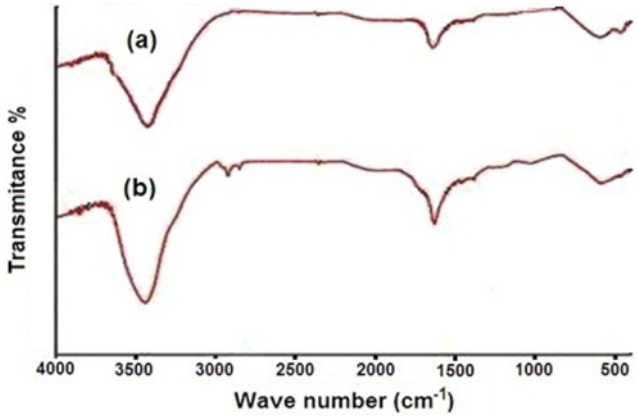

Fig. 3. FTIR spectra of (a) prepared MWCNTs (b) oxidized MWCNTs.

assigned to the stretching vibrations of -OH, >C=O group [22,23]. New bands (2,924 and 2,848 cm^{-1}) appeared in Oxidized MWCNTs due to -C-H stretching vibration [24]. For this sample the functional groups may come from the acid washing to remove the catalyst when being fabricated or the weak oxidation in air. The broad band

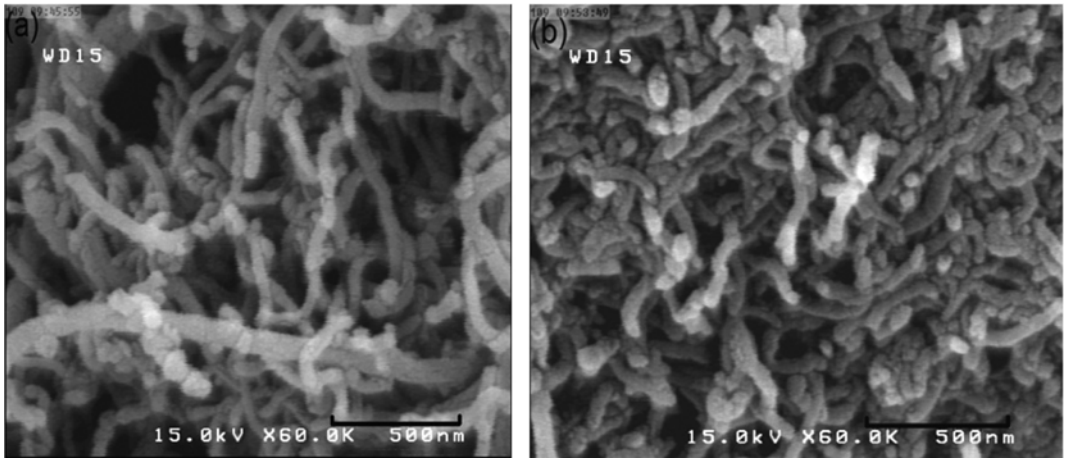

Fig. 1. SEM picture of (a) prepared MWCNTs (b) oxidized MWCNTs.

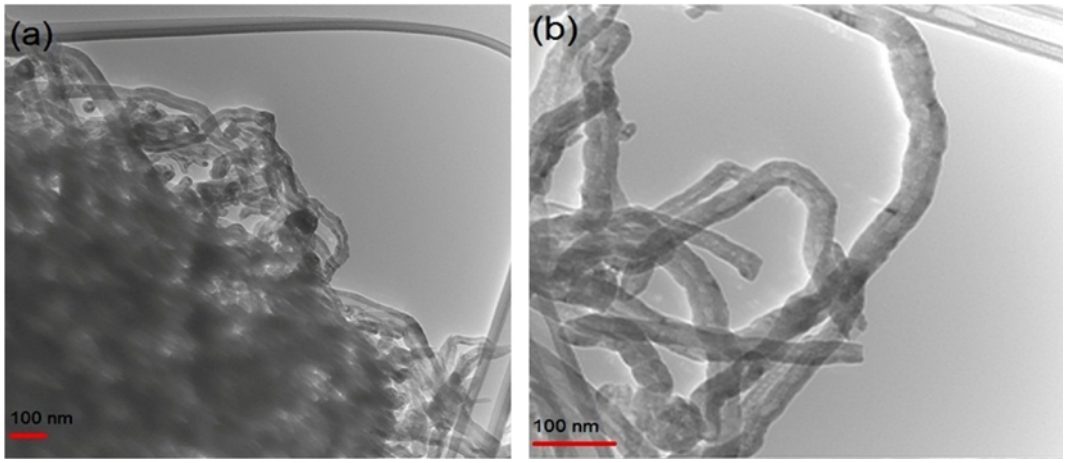

Fig. 2. TEM picture of (a) prepared MWCNTs (b) oxidized MWCNTs.

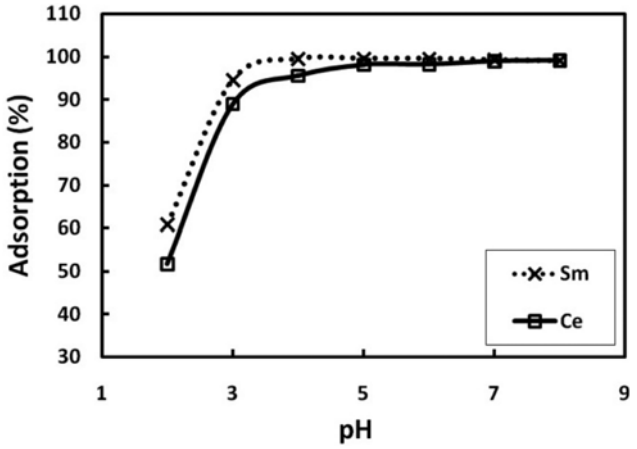

Fig. 4. Effect of pH on the adsorption of Ce(III) and Sm(III) ions on oxidized MWCNTs (C_0=10 mg/L, contact time=120 min, adsorbent dosage=1 g/L, temperature=30 °C).

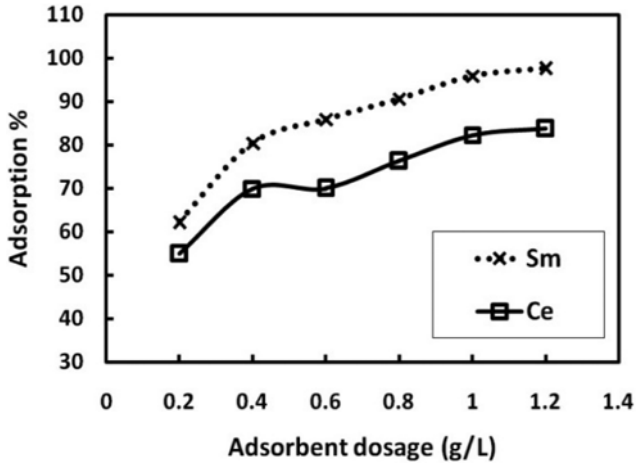

Fig. 5. Effect of adsorbent dosage on the adsorption of Ce(III) and Sm(III) ions on oxidized MWCNTs (C_0=20 mg/L, contact time=120 min, pH=5, temperature=30 °C).

at over 3,000 cm^{-1} represents hydroxyl groups. Therefore, on the surface of our materials oxygen-containing functional groups such as hydroxyl, carboxyl and carbonyl groups are present in detectable quantity, even on the initial MWCNTs. This group is expected to be the active centers for metal cations [25].

2. Effect of pH

It is well-known that the pH of solution has an important role in sorption of metal ions by MWCNTs. It affects the activity of the functional groups present in the adsorbent that are responsible for metal adsorption and also affects the composition of metallic ions to get adsorbed to the active sites [26]. The percentage of metal ions removed from solution versus pH is shown in Fig. 4. At low pH values (pH<3), the low adsorption can be explained by the increase in positive charge density on the surface sites and, thus, electrostatic repulsion occurs between the metal ions and the edge group with positive charge on the surface of oxidized MWCNTs [27,28].

At higher pH values (3<pH<6), the surface of oxidized MWCNTs becomes negatively charged and thus electrostatic repulsion decreases with an increase in pH value. The reduction of positive charge density on the sorption edges results in an increase in the metal adsorption. More increase in pH values leads to metal precipitation, and metal accumulation on oxidized MWCNTs surface deteriorated the adsorption mechanism. Therefore, kinetic studies above pH 6 were not attempted due to the precipitation of metal ions as hydroxides. The most adsorption percentage for both of Ce(III) and Sm(III) occurred at 5<pH<6. Therefore, all experiments were carried out at pH 5.

3. Effect of Adsorbent Dosage

One of the parameters that strongly affects sorption capacity is the quantity of the contacting sorbent in the liquid phase. The effect of the adsorbent dosage on the sorption of Ce(III) and Sm(III) is shown in Fig. 5. This figure shows that the sorption efficiency increases with an increase in adsorbent dosage. This is expected because of the availability of more binding sites and making easier penetration of metal ions to the sorption sites. This figure indicates that the adsorption percentage becomes almost constant at 1 g/L for Ce(III) and Sm(III) ions and this is used for all further experiments.

4. Adsorption Isotherms

Adsorption isotherms are important for the description of how molecules or ions of adsorbate interact with adsorbent surface sites, and also, are critical in optimizing the use of adsorbent. The experimental data for Ce(III) and Sm(III) ions adsorption onto the oxidized MWCNTs were analyzed using Langmuir, Freundlich and Dubinin-Radushkevich (D-R) isotherms.

The Langmuir isotherm was used successfully to characterize the monolayer adsorption process. This model can be expressed in a linear from as follows [29]:

$$\frac{C_e}{q_e}=\frac{1}{K_L q_m}+\frac{C_e}{q_m} \tag{6}$$

Where q_e is the equilibrium adsorption uptake of Ce(III) and Sm (III) ions, in mg/g, C_e is the equilibrium concentration of Ce(III) and Sm(III) ions, in mg/L, q_m is the maximum adsorption uptake capacity corresponding to the complete monolayer coverage, in mg/g, and K_L is the Langmuir sorption constant relating the free energy of sorption, in L/mg.

The essential characteristic of a Langmuir isotherm can be expressed in terms of dimensionless separation factor or equilibrium parameter R_L, which is defined as:

$$R_L=\frac{1}{1+K_L C_0} \tag{7}$$

Where K_L is the Langmuir constant and C_0 is the initial Ce(III) and Sm(III) ions concentration, in mg/L. the value of R_L indicates the type of the isotherm to be either unfavorable (R_L>1), linear (R_L=1), favorable (0<R_L<1) or irreversible (R_L=0).

The Freundlich isotherm model proposes a sorption with a heterogeneous energetic distribution of active sites, accompanied by interactions between adsorbed molecules. It can be presented in a linear form as follows [18]:

$$\log q_e=n\log C_e+\log K_F \tag{8}$$

where q_e is the equilibrium adsorption uptake of Ce(III) and Sm(III) ions, in mg/g, C_e is the equilibrium concentration of Ce(III) and Sm (III) ions, in mg/L, and K_F and n are the Freundlich parameters related

to adsorption capacity and adsorption intensity, respectively.

The D-R isotherm model is valid at low concentration ranges and can be used to describe adsorption on both homogeneous and heterogeneous surfaces. The linear form of D-R equation is expressed in the following equation [18]:

$$\ln q = \ln q_{max} - \beta\varepsilon^2 \quad (9)$$

The Polanyi potential (ε) is equal to:

$$\varepsilon = RT\ln\left(1+\frac{1}{C_e}\right) \quad (10)$$

Where q_e is the equilibrium adsorption uptake of Ce(III) and Sm (III) ions, in mol/g, q_m is the maximum adsorption capacity corresponding to the complete monolayer coverage, in mol/g, ε is the Polanyi potential, β is the activity coefficient related to mean adsorption energy, in mol^2/kJ^2, R is the ideal gas constant, in 8.3145 J/mol·K, T is the absolute temperature, in Kelvin, C_{eq} is the equilibrium concentration of Ce(III) and Sm(III) ions, in mol/L. E is defined as the free energy change (kJ/mol), which requires transferring 1 mol of ions from solution to the solid surfaces. The relation is as follows:

$$E = \frac{1}{\sqrt{2\beta}} \quad (11)$$

Table 2. Parameters of adsorption isotherm models of Ce(III) and Sm(III) onto oxidized MWCNTs

Adsorption isotherm model	Isotherm constants	Metal ions	
		Sm(III)	Ce(III)
Langmuir model	q_m (mg/g)	89.28	92.59
	K_L (L/mg)	0.057	0.0614
	R_L	0.09-0.66	0.08-0.58
	R^2	0.8193	0.8597
	AARE %	42.14	26.71
Freundlich model	n	0.3249	0.3581
	K_F (L/g)	16.0879	15.3073
	R^2	0.9585	0.9616
	AARE %	13.86	12.57
D-R model	q_{max} (mol/g)$\times 10^4$	9.9507	13.5955
	q_{max} (mg/g)	149.62	190.49
	β (mol^2/kJ^2)	0.0024	0.0028
	E (kJ/mol)	14.43	13.36
	R^2	0.9375	0.9401
	AARE %	16.28	15.43

The magnitude of E is useful for estimating the mechanism of the adsorption reaction. The adsorption is dominated by chemical ion-exchange if E is in the range of 8-16 kJ/mol, whereas physical forces may affect the adsorption in the case of E<8 kJ/mol [30,31].

The Langmuir, Freundlich and D-R model constants, along with the correlation coefficient (R^2) and AARE (%) values are presented in Table 2. The sorption of Ce(III) and Sm(III) ions onto oxidized MWCNTs is fitted better to the Freundlich isotherm model. The R_L values range from 0.09 to 0.66 for Sm(III) and 0.08 to 0.58 for Ce(III) ions. These values show that the sorption of Ce(III) and Sm (III) ions onto oxidized MWCNTs is favorable within the experimental condition studied. The value of K_F calculated from the Freundlich model is large, which indicates that oxidized MWCNTs have a high adsorption affinity towards Ce(III) and Sm(III). The deviation of n from unity indicates a non-linear adsorption that takes place on the heterogeneous surfaces. The E values obtained from Eq. (11) are 14.43 and 13.36 kJ/mol for Sm(III) and Ce(III), respectively, which are in the adsorption energy range of chemical ion-exchange reaction. This suggests that Ce(III) and Sm(III) adsorption onto oxidized MWCNTs is attributed to chemical adsorption rather than physical adsorption. The maximum uptake capacities (q_m) calculated by applying the D-R model for samarium and cerium ions are found to be 149.62 and 190.49 (mg/g), respectively. The pH values of the suspension before and after the adsorption of Ce(III) and Sm(III) in each test tube measured. It is interesting that the initial pH of the suspension is about 5, whereas the final pH values of the suspensions for Ce(III) and Sm(III) are about 4.5 and 4.6, respectively. In the adsorption processes, Ce(III) and Sm(III) ions substitute for H^+ of functional groups on the oxidized MWCNTs. The H^+ is released from the oxidized MWCNTs into the solution, and thus the pH values decrease after equilibration. The maximum adsorption capacity of oxidized MWCNTs for Ce(III) and Sm(III) ions obtained in this study is compared with other adsorbents on Langmuir isotherm model basis as shown in Table 3. According to this data, the sorption capacity of the oxidized MWCNTs for cerium and samarium is relatively high.

5. Adsorption Kinetics

To examine the controlling mechanism of the sorption process, kinetic models are used to test the experimental data. Three simplified kinetics, namely pseudo-first-order, pseudo-second-order and intra-particle diffusion models, are applied for the experimental data to predict the adsorption kinetics. The pseudo-first-order equation is one the most widely used rate equations to describe the adsorption of an adsorbate from the liquid phase. The non-linear pseudo-first-order equation is given as follows [27]:

Table 3. Comparison of adsorption potential of various adsorbents for samarium and cerium removal from aqueous solution

Adsorbent	Samarium q_m (mg/g)	Cerium q_m (mg/g)	References
Brown Marine Alga, Turbinaria Conoides	-	152.8	32
Pinus brutia leaf powder	-	17.24	11
Platanus orientalis leaf powder	-	32.05	12
Modified Pinus brutia leaf powder	-	62.1	33
Bentonite modified with N-(2-hydroxyethyl) ethylenediamine	17.7	-	34
Sargassum biomass	97.5	-	35
Multi walled carbon nanotubes	89.28	92.59	This work

$$q_t = q_e(1 - e^{-k_1 t}) \quad (12)$$

Where q_e and q_t, in mg/g, are the amount of metal ions adsorbed at equilibrium and at time t, in min, respectively and k_1 is the pseudo-first-order rate constant, in min^{-1}.

The pseudo-second-order model is more suitable for the description of the kinetic behavior of adsorption in which chemical sorption is the rate-controlling step [27]. The pseudo-second-order model [36] is expressed by:

$$\frac{t}{q_t} = \frac{1}{k_2 q_e^2} + \frac{t}{q_e} \quad (13)$$

Where k_2 is the rate constant of the pseudo-second-order equation, in g/mg.min.

The kinetic results were analyzed by the intra-particle diffusion model [37] in order to elucidate the diffusion mechanism. The intra-particle diffusion model is expressed by:

$$q_t = k_p t^{0.5} + C \quad (14)$$

Where k_p is the intra-particle diffusion rate constant, in mg/g·$min^{0.5}$, and C, in mg/g, is a constant related to the thickness of the boundary layer. According to this model, if the plot of q_t versus $t^{0.5}$ gives a straight line, then intra-particle diffusion is involved in the adsorption process; and if this line passes through the origin then intra-particle diffusion is the rate-controlling step [38]. However, if the data present multi-linear plots, then two or more steps influence the adsorption process such as external diffusion, intra-particle diffusion etc. [39].

The values of rate constant along with correlation coefficient and AARE values are presented in Tables 4 and 5. The AARE values are 6% and 6.9% for the pseudo-first-order model and 2.73% and 2.54% for pseudo-second-order model, indicating a better fit with the pseudo-second-order model. The consistency of the experimental data with the pseudo-second-order kinetic model indicates that the adsorption of Ce(III) and Sm(III) ions on oxidized MWCNTs is controlled by chemical adsorption (chemisorption) involving valence forces through sharing or exchange electrons between sorbent and sorbate [39]. In chemical adsorption, it is assumed that the adsorption capacity is proportional to the number of active sites occupied on the adsorbent surface [36,37,40].

Table 4. Parameters of the kinetic models for sorption of Ce(III) and Sm(III) ions onto oxidized MWCNTs

	Pseudo-first-order kinetic model			
Metal ions	k_1 (min^{-1})	q_e (mg/g)	R^2	AARE %
Sm(III)	14.06	0.1085	0.8682	6
Ce(III)	16.57	0.2441	0.553	6.09
	Pseudo-second-order kinetic model			
Metal ions	k_2 (g/mg·min)	q_e (mg/g)	R^2	AARE %
Sm(III)	15.625	0.0101	0.9991	2.73
Ce(III)	18.018	0.0177	0.9996	2.54

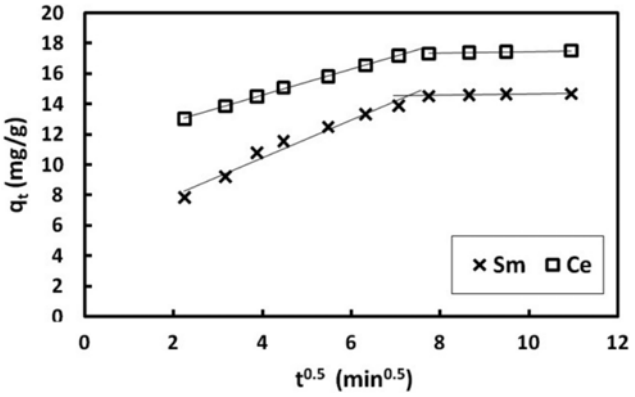

Fig. 6. Intra-particle diffusion model for sorption of Ce(III) and Sm(III) ions onto oxidized MWCNTs (pH=5, adsorbent dosage=1 g/L, temperature=30 °C).

As can be observed in Fig. 6, the data points are related by two straight lines. The first sharper portion is attributed to the diffusion of adsorbate through the solution to the external surface of the adsorbent (external diffusion), and the second portion describes the gradual adsorption stage, corresponding to diffusion of adsorbate molecules inside the pores of the adsorbent (intra-particle diffusion) [39]. The results obtained demonstrate that adsorption of Ce(III) and Sm(III) ions on oxidized MWCNTs is controlled by chemical adsorption, external diffusion and to some extent intra-particle diffusion.

6. Adsorption Thermodynamics

Thermodynamic behavior of the sorption of Sm(III) and Ce(III) ions onto MWCNTs is investigated using the thermodynamic parameters that include the change in free energy (ΔG^o), enthalpy (ΔH^o) and entropy (ΔS^o). These parameters are calculated from the following equations:

$$\ln K_d = \frac{\Delta S^o}{R} - \frac{\Delta H^o}{RT} \quad (15)$$

Where K_d is the distribution coefficient (mL/g), ΔH^o is the enthalpy change, ΔS^o is the entropy change, T is the temperature (K), and R is the ideal gas constant. The free energy change (ΔG^o) is determined using the following equation:

$$\Delta G^o = \Delta H^o - T\Delta S^o \quad (16)$$

Based on Eq. (15), the ΔH^o and ΔS^o parameters can be calculated from the slope and intercept of the plot of $\ln K_d$ vs. 1/T, respectively (Fig. 7). The values of ΔG^o, ΔH^o and ΔS^o are given in Table 6 for Ce(III) and Sm(III) sorption onto oxidized MWCNTs. The negative values of ΔG^o indicate thermodynamically feasible and spontaneous nature of the sorption. The negative values of ΔH^o confirm the exothermic nature of sorption process of both metal ions

Table 5. Parameters of intra-particle diffusion model for sorption of Ce(III) and Sm(III) ions onto oxidized MWCNTs

Metal ions	K_{P1} (mg/g·$min^{0.5}$)	C_1	R^2	K_{P2} (mg/g·$min^{0.5}$)	C_2	R^2
Sm(III)	1.2487	5.4588	0.9687	0.0428	14.218	0.8743
Ce(III)	0.8534	11.158	0.9988	0.0558	16.893	0.9933

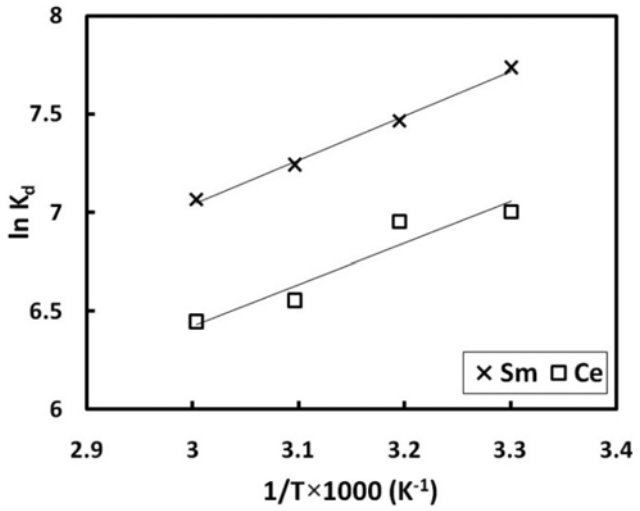

Fig. 7. Plots of ln K_d vs. 1/T for cerium and samarium sorption onto oxidized MWCNTs (pH=5, adsorbent dosage=1 g/L).

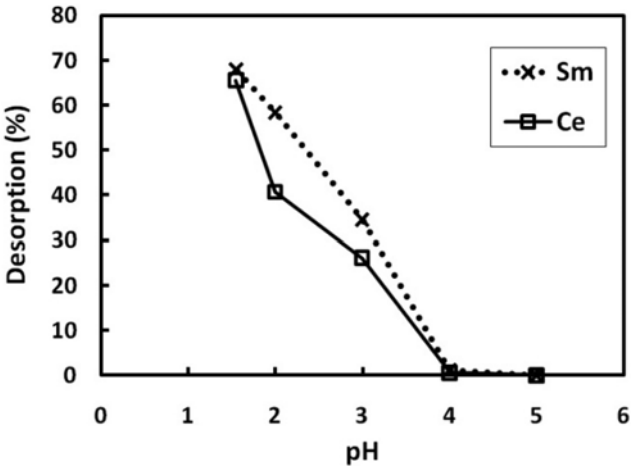

Fig. 8. Desorption of Ce(III) and Sm(III) ions from oxidized MWCNTs at different pH values of the solution (C_0=20 mg/L, adsorbent dosage=1 g/L, temperature=30 °C).

onto oxidized MWCNTs. The positive ΔS^o values indicate the affinity of the sorbent for the both metal ions.

7. Desorption

The repeated availability of MWCNTs is a crucial factor for applying them in removal of Sm(III) and Ce(III) from a large volume of solution in real work. So, the desorption of adsorbed Sm(III) and Ce(III) from MWCNTs was studied also. The Ce(III) and Sm(III) desorption curves with different pH values of solution are shown in Fig. 8. The desorption percentage is almost zero when the pH of solution is 5.0. It is obvious that the Ce(III) and Sm(III) desorption increases with the decrease of pH value of the solution. At pH 4.0, desorption percentage increases sharply and at pH 1.55, eventually reaches 70%. These results indicate that the Ce(III) and Sm(III) adsorbed by oxidized MWCNTs can be easily desorbed, so the oxidized MWCNTs can be employed repeatedly in adsorption of lanthanides, which will remarkably reduce the overall cost for the adsorbent.

CONCLUSIONS

The adsorption of Ce(III) and Sm(III) from aqueous solution onto oxidized MWCNTs was investigated. The greatest adsorption percentage for both Ce(III) and Sm(III) occurred at 5<pH<6. The adsorption percentage becomes almost constant at 1 g/L for Ce(III) and Sm(III) ions. The sorption of Ce(III) and Sm(III) ions onto oxidized MWCNTs is fitted better to the Freundlich isotherm model than that of the Langmuir and D-R isotherm models. The maximum uptake capacities (q_m) calculated by applying the D-R model for samarium and cerium ions are found to be 149.62 and 190.49 (mg/g), respectively. The adsorption of Ce(III) and Sm(III) may be dominated by chemical adsorption and ion-exchange. The diffusion of adsorbate through the solution is attributed to external and intra-particle diffusion. The negative values of ΔG^o indicate the spontaneous nature of the sorption. The negative values of ΔH^o demonstrate that the sorption of both metal ions onto oxidized MWCNTs in the temperature range of 30-60 °C was exothermic. The positive ΔS^o values indicate the increase of randomness at the solid/liquid interface during the adsorption process for the both metal ions.

Most of the adsorbed Ce(III) and Sm(III) can be easily desorbed from MWCNTs by decreasing the solution pH values. Thus, oxidized MWCNTs were considered to be effective and promising materials for the removal of both Ce(III) and Sm(III) from wastewater.

REFERENCES

1. K. Kondo and E. Kamio, *Desalination*, **144**, 249 (2002).
2. T. P. Rao and V. M. Biju, *Crit. Rev. Anal. Chem*., **30,** 179 (2000).
3. L. Jelinek, Y. Z. Wei and M. Kumagai, *J. Rare Earths*, **24**, 385 (2006).
4. I. G. Finlay, M. D. Mason and M. Shelley, *The Lancet Oncol*., **6**, 392 (2005).
5. A. Trovarelli, *Catalysis by ceria and related materials*, World Scientific Publishing Company (2002).
6. L. Zuo, S. Yu, H. Zhou, J. Jiang and X. Tian, *J. Radioanal. Nucl. Chem*., **288**, 579 (2011).
7. F. Fu and Q. Wang, *J. Environ. Manage*., **92**, 407 (2011).
8. S. Chakravarty, A. Mohanty, T. Nag Sudha, A. K. Upadhyay, J. Konar, J. K. Sircar, A. Madhukar and K. K. Gupta, *J. Hazard.*

Table 6. Thermodynamic parameters for the sorption of samarium and cerium ions onto Oxidized MWCNTs

	ΔG^o (kJ/mol)				ΔH^o (kJ/mol)	ΔS^o (J/mol·K)
Metal ions	30 °C	40 °C	50 °C	60 °C		
Sm(III)	−19.4424	−19.4669	−19.4914	−19.5159	−18.7	2.45
Ce(III)	−17.7682	−17.7787	−17.7892	−17.7997	−17.45	1.05

Mater., **173**, 502 (2010).
9. M. Rafatullah, O. Sulaiman, R. Hashim and A. Ahmad, *J. Hazard. Mater*., **170**, 969 (2009).
10. D. Wu, J. Zhao, L. Zhang, Q. Wu and Y. Yang, *Hydrometallurgy*, **101**, 76 (2010).
11. C. Kutahyali, S. Sert, B. Cetinkaya, S. Inan and M. Eral, *Sep. Sci. Technol*., **45**, 1456 (2010).
12. S. Sert, C. Kutahyali, B. Cetinkaya, Z. Talip, S. Inan and M. Eral, *Hydrometallurgy*, **90**, 13 (2008).
13. R. C. Oliveira, E. Guibal and O. Garcia Jr., *Biotechnol. Prog*., **28**, 715 (2012).
14. V. K. Gupta, A. Rastogi and A. Nayak, *J. Colloid Interface Sci*., **342**, 135 (2010).
15. S. Iijima, *Nature (London)*, **354**, 56 (1991).
16. C. L. Chen and X. K. Wang, *Ind. Eng. Chem. Res.*, **45**, 9144 (2006).
17. G. D. Sheng, D. D. Shao, X. M. Ren, X. Q. Wang, J. X. Li, Y. X. Chen and X. K. Wang, *J. Hazard. Mater.*, **178**, 505 (2010).
18. X. L. Tan, D. Xu, C. L. Chen, X. K. Wang and W. P. Hu, *Radiochim. Acta*, **96**, 23 (2008).
19. S. Yang, J. Li, D. Shao, J. Hu and X. K. Wang, *J. Hazard. Mater*., **166**, 109 (2009).
20. Q. H. Fan, D. D. Shao, J. Hu, C. L. Chen, W. S. Wu and X. K. Wang, *Radiochim. Acta*., **97**, 141 (2009).
21. X. Wang, C. Chen, W. Hu, A. P. Ding, D. Xu and X. Zhou, *Environ. Sci. Technol*., **39**, 2856 (2005).
22. C. L. Chen, J. Hu, D. Xu, X. Tan, Y. Meng and X. K. Wang, *J. Colloid Interface Sci*., **323**, 33 (2008).
23. G. Y. Li, Y. R. Jiang, K. L. Huang, P. Ding and L. L. Yao, *Colloids Surf*.: *A*, **320**, 11 (2008).
24. Z. Zang, Z. Hu, Z. Li, Q. He and X. Chang, *J. Hazard. Mater*., **172**, 958 (2009).
25. Z. Gao, T. J. Bandosz, Z. Zhao, M. Han and J. Qiu, *J. Hazard. Mater*., **167**, 357 (2009).
26. N. Feng, X. Guo, S. Liang, Y. Zhu and J. Liu, *J. Hazard. Mater*., **185**, 49 (2011).
27. A. Sari, M. Tuzen, D. Citak and M. Soylak, *J. Hazard. Mater.*, **148**, 387 (2007).
28. H. Ghassabzadeh, A. Mohadespour, M. Torab-Mostaedi, P. Zaheri, M. G. Maragheh and H. Taheri, *J. Hazard. Mater*., **177**, 950 (2010).
29. I. Langmuir, *J. Am. Chem. Soc*., **40**, 1361 (1918).
30. R. Donat, A. Akdogan, E. Erdem and H. Cetisli, *J. Colloid Interface Sci*., **286**, 43 (2005).
31. A. Ozcan, E. M. Oncu and A. S. Ozcan, *Colloids Surf.: A*, **277**, 90 (2006).
32. K. Vijayaraghavan, M. Sathishkumar and R. Balasubramanian, *Ind. Eng. Chem. Res*., **49**, 4405 (2010).
33. C. Kütahyali, Ş. Sert, B. Çetinkaya, E. Yalçıntaş, M. B. Acar, *Wood Sci. Technol*., **46**, 721 (2012).
34. D. Li, X. Chang, Z. Hu, Q. Wang, R. Li and X. Chai, *Talanta*, **83**, 1742 (2011).
35. R. C. Oliveira, C. Houannin, E. Guibal and O. Garcia Jr., *Process Biochem*., **46**, 736 (2011).
36. Y. S. Ho and G. McKay, *Process Biochem*., **34**, 451 (1999).
37. M. A. Tofighy and T. Mohammadi, *J. Hazard. Mater*., **185**, 140 (2011).
38. J. P. Chen, S. Wu and K. H. Chong, *Carbon*, **41**, 1979 (2003).
39. S. Figaro, J. P. Avril, F. Brouers, A. Ouensanga and S. Gaspard, *J. Hazard. Mater*., **161**, 649 (2009).
40. W. Zou, R. Han, Z. Chen, Z. Jinghua and J. Shi, *Colloids Surf.: A*, **279**, 238 (2006).